iScience, Volume *23*

Supplemental Information

Inositol 1,4,5-Trisphosphate Receptor Type 3 Regulates Neuronal Growth Cone Sensitivity to Guidance Signals

Carmen Chan, Noriko Ooashi, Hiroki Akiyama, Tetsuko Fukuda, Mariko Inoue, Toru Matsu-ura, Tomomi Shimogori, Katsuhiko Mikoshiba, and Hiroyuki Kamiguchi

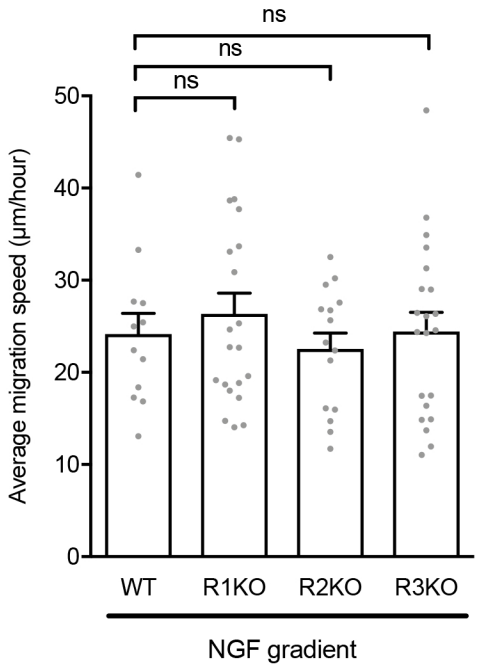

Figure S1. Growth cone migration speed in NGF gradients. Related to Figure 1.
WT and IP_3R subtype-specific knockout growth cones migrating in NGF gradients were observed under differential interference contrast microscopy, and the average displacement of the central domain distal edge was quantified and expressed as micrometers per hour. Bars represent mean ± SEM, with each gray dot indicating data from a single growth cone. ns, not significant; Dunnett's test.

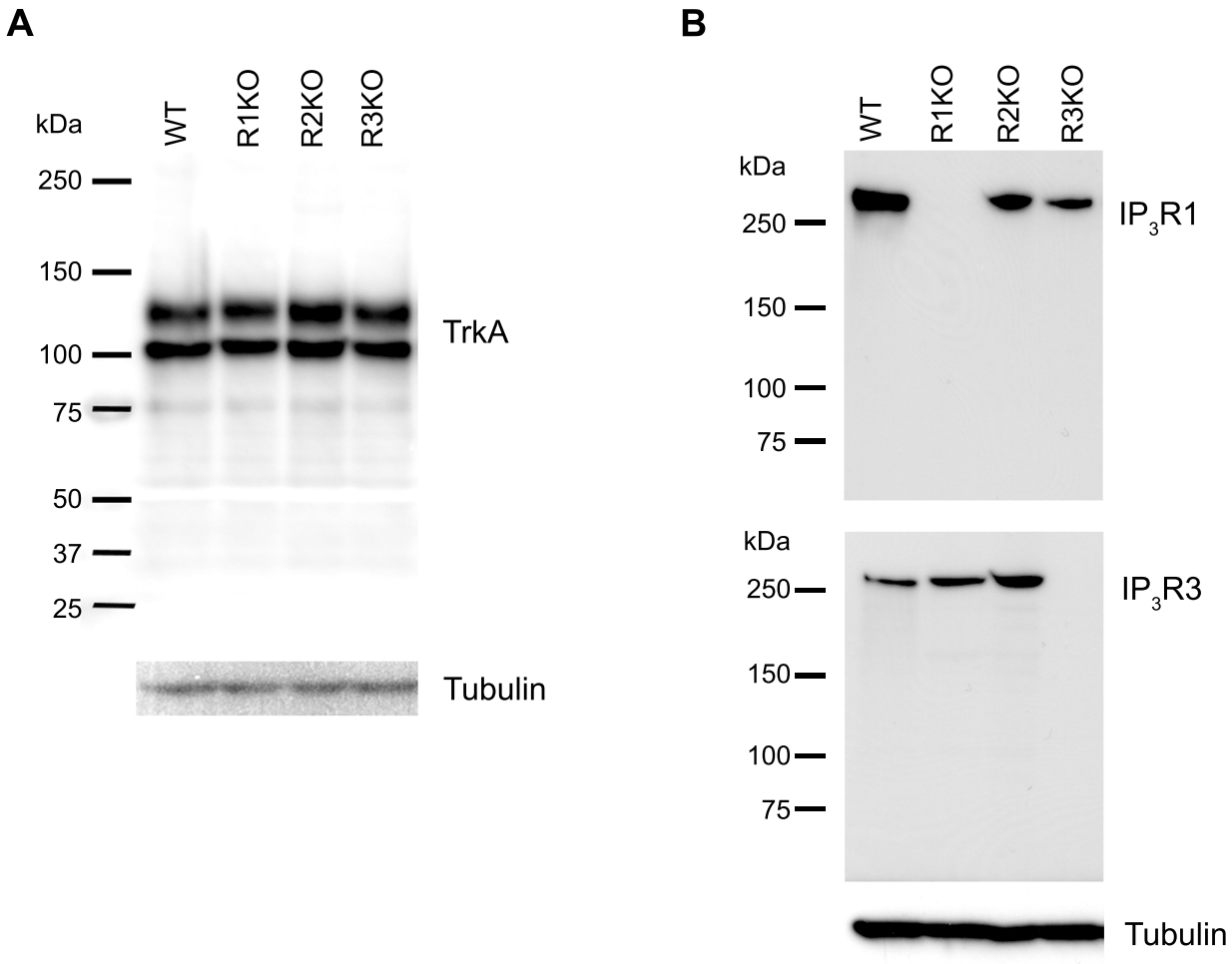

Figure S2. Western blot analysis of TrkA and IP_3R subtypes. Related to Figures 2 and 3.
(A) Shown are TrkA and tubulin (loading control) in DRGs of WT and IP_3R subtype-specific knockout mice. According to a previous report (Barker et al., 1993), the anti-TrkA antibody used here can detect both TrkA full-length protein at approximately 140 kDa and an isoform of glycosylated TrkA at approximately 110 kDa.
(B) Shown are IP_3R1, IP_3R3 and tubulin (loading control) in DRGs of WT and IP_3R subtype-specific knockout mice.

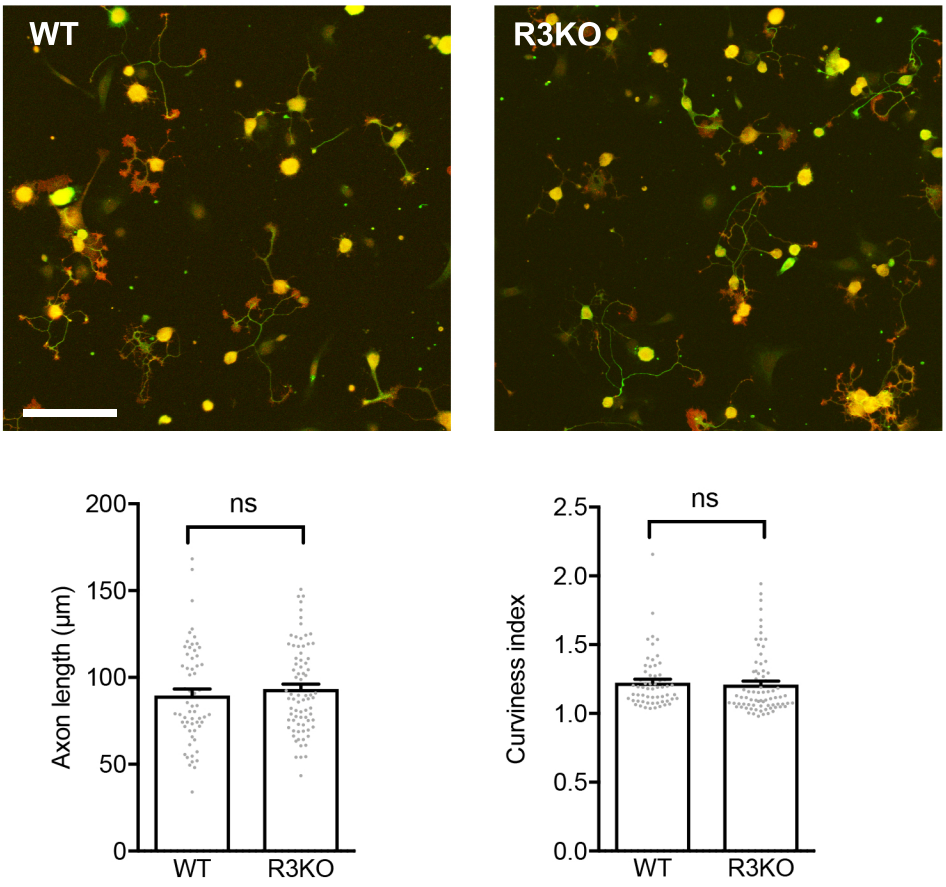

Figure S3. Directional axon growth from WT and R3KO neurons. Related to Figure 7.
WT or R3KO DRG neurons cultured on poly-D-lysine substrates for five hours were fixed and immunostained for neuronal tubulin (green) and TrkA (red). Scale bar, 100 μm. Between WT and R3KO neurons, neither axon length nor curviness index showed statistically significant difference by Student's *t* test. Numbers in brackets represent the number of axons included in each group. Data are represented as mean ± SEM.

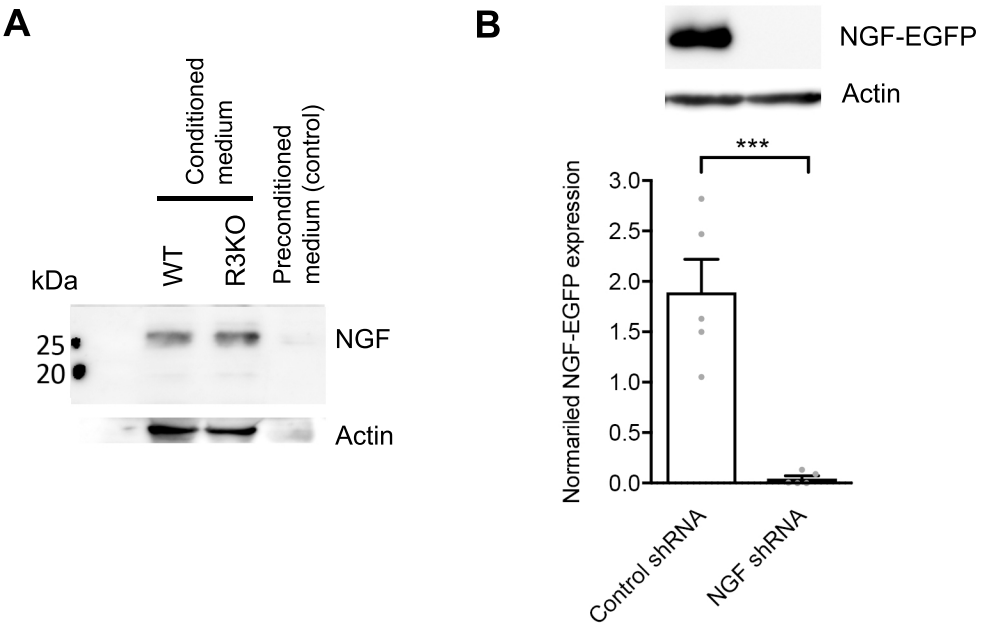

Figure S4. NGF release from keratinocytes and its downregulation by shRNA. Related to Figures 7 and 8. (A) Skin keratinocyte cultures were prepared from Wt and R3KO mice. Four days after plating, 60 mL of conditioned medium was concentrated to 200 µL using Amicon columns according to manufacturer's protocol. The concentrated medium was processed for Western blotting to detect endogenous NGF and actin as a loading control. (B) The effect of NGF shRNA on NGF expression was assessed in keratinocytes transfected with a construct coding NGF-EGFP fusion protein. NGF-EGFP expression was quantified by immunoblotting with GFP antibodies (Santa Cruz, sc-9996; 1/1000 overnight at 4°C). The graph shows NGF-EGFP normalized to actin. Bars represent mean ± SEM, with each gray dot indicating data from each of 5 independent experiments. *** $p < 0.001$; Student's *t* test.

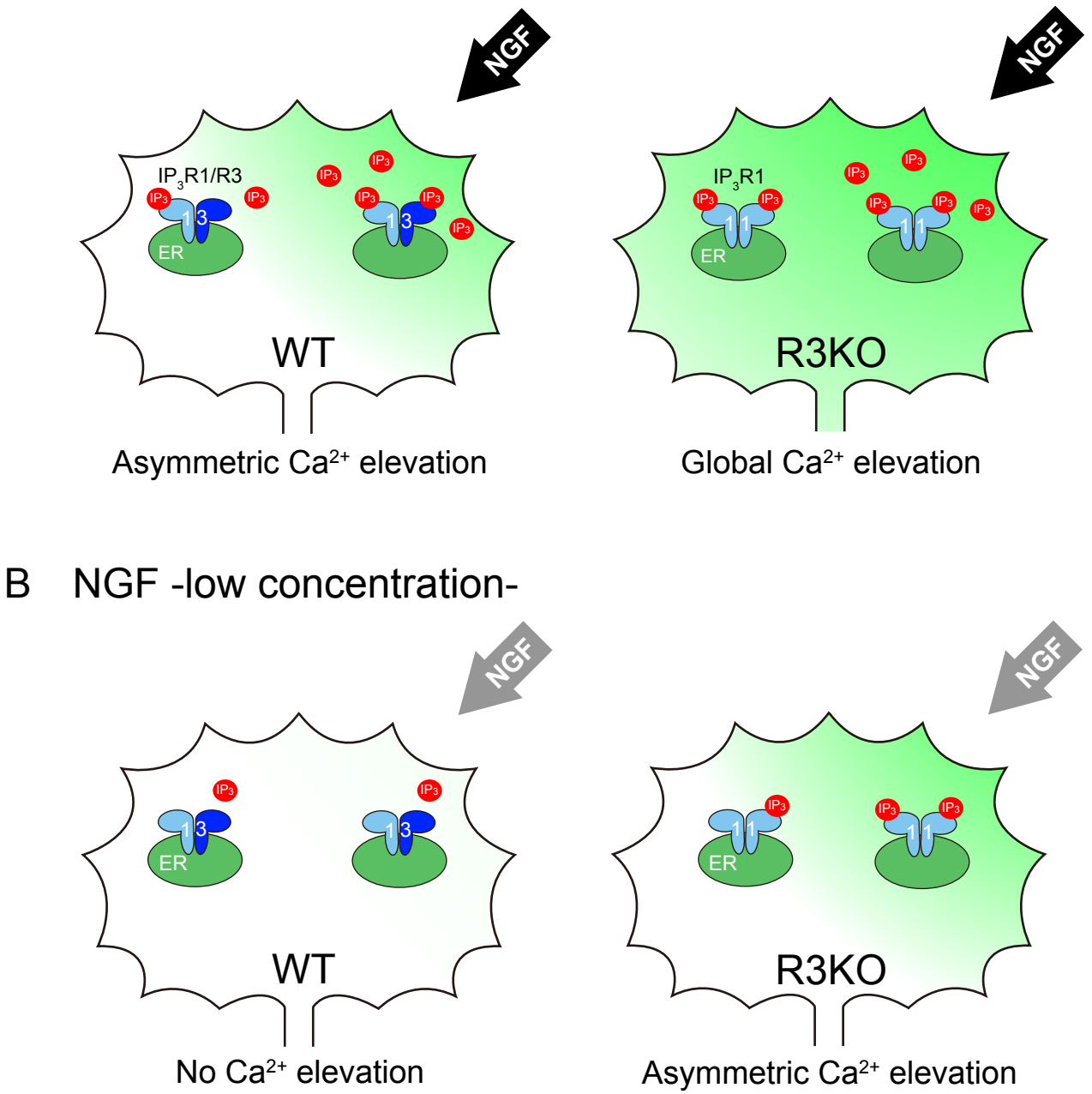

Figure S5. **Model of IP_3R3 involvement in the regulation of growth cone sensitivity to guidance signals**.
(A) An extracellular NGF gradient (arrow) evokes the production of IP_3 (red) on the near side of the growth cone. The localized IP_3 elevation in turn causes IICR (green) only on the near side of WT growth cone or on both sides of R3KO growth cone. In WT, type 3 subunit ('3') forms tetrameric IP_3Rs with relatively low IP_3 affinity. As a result, these IP_3Rs can confine IICR to the near side even in the presence of small amounts of far-side IP_3 that are produced locally or diffused from the near side. In R3KO, however, the low levels of IP_3 on the far side are above the threshold required to activate IP_3Rs that consist exclusively of the higher-affinity type 1 subunit ('1'). Such abnormal IICR on the far side abolishes Ca^{2+} signal asymmetry, therefore renders R3KO growth cones irresponsive to normal concentration ranges of NGF that can attract WT growth cones.
(B) When extracellular NGF concentration is too low, WT growth cone cannot generate Ca^{2+} signals even on the near side. Therefore, they fail to recognize such a low level of NGF as an attractive cue. By contrast, hypersensitive IP_3R in R3KO growth cone can generate IICR on the near side, and this growth cone can turn toward lower-than-threshold NGF required for WT growth cone turning.

Transparent Methods

Mice

R1KO, R2KO and R3KO mice (Futatsugi et al., 2005; Matsumoto et al., 1996) were maintained at the RIKEN Center for Brain Science Animal Care Facility. The experimental procedures and housing conditions for animals were approved by the Wako Animal Experiments Committee at RIKEN, and all of the animals were cared for and treated humanely in accordance with the Institutional Guidelines for Experiments Using Animals. Postnatal day 0 mice were used without sex determination.

Western blotting

DRGs were homogenized by sonication in lysis buffer as described (Wada et al., 2016). DRG lysate proteins were separated by SDS-PAGE and transferred to PVDF membranes (Merck Millipore). After blocking with 5% skim milk and 0.1% Tween 20 in PBS at room temperature for 1 hour, the membranes were incubated at 4°C overnight with anti-TrkA (R&D) anti-IP_3R1 (4C11; Otsu et al., 1990), anti-IP_3R3 (BD Biosciences) and anti-tubulin antibodies (Covance/Biolegend). After incubation with HRP-conjugated secondary antibodies, bands were visualized with chemiluminescent substrate solutions (Pierce™ ECL Western Blotting Substrate; Thermo Fisher Scientific). For immunoblotting of multiple IP_3R subtypes, the membranes were stripped with stripping buffer (Restore™ Western Blot Stripping Buffer; Thermo Fisher Scientific) before incubation with a different primary antibody.

Cell culture

DRGs dissected from postnatal day 0 mice were dissociated and plated on a glass-based dish coated with poly-D-lysine and 10 μg/ml laminin (Life Technologies). The cells were incubated at 37°C in RPMI-1640 medium (Invitrogen) supplemented with 10% fetal bovine serum and 10 ng/ml NGF (Promega) for 2 hours. The medium was then changed to serum-free Neurobasal®-A (Invitrogen) supplemented with B-27 (Invitrogen) before starting experiments.

Growth cone turning assay

Assays of growth cone turning induced by FLIP of caged IP_3 were performed as described previously (Akiyama et al., 2009). Briefly, DRG neurons were loaded with a caged IP_3 derivative (iso-Ins(1,4,5)P_3/PM; 0.5 μM or 0.1 μM in media; Alexis Biochemicals) and 0.02% Cremophor EL (Sigma-Aldrich) in L15 medium (Life Technologies) for 30 min and then washed with L15 alone. Afterwards the cells were incubated with NGF-containing L15 for at least 30 min before the start of experiments. Spatially restricted IP_3 signals were generated by repetitive FLIP every three seconds. Differential interference contrast images of growth cones were acquired before and up to 30 min after the start of repetitive FLIP.

Assays of growth cone turning induced by a microscopic gradient of NGF (0.025 to 50 μg/ml in pipette) or MAG (150 μg/ml in pipette; R&D systems) were performed as described previously (Hong et al., 2000; Lohof et al., 1992). The gradient was produced by pulsatile pressure ejection of NGF or MAG from a micropipette positioned at a 45° angle 100 μm from the growth cone. The turning angle was defined as the difference in growth cone migration direction before and 40 minutes after the start of pulsatile ejection of guidance molecules.

Ca^{2+} imaging

For imaging IP_3-induced Ca^{2+} elevations, we used the fluorescent Ca^{2+} indicator Fluo-8H (4μM, AAT Bioquest). For quantitative analysis, two ROIs were positioned on each growth cone: the near side ROI defined as a circular region whose center corresponded to the site of laser irradiation and whose diameter equaled to one-third of the width of each growth cone; the far side ROI defined as a circular region of the same diameter that was placed on the center of the far-side half of each growth cone. The averaged Fluo-8H fluorescence intensity within each ROI (F) at each time point was normalized to the baseline Fluo-8H intensity (F_{base}), the averaged F before the onset of FLIP of IP_3. Then, the ratio F/F_{base} (defined as F') was used as a measure of cytosolic Ca^{2+} signals.

For imaging NGF-induced Ca^{2+} elevations, DRG neurons were preloaded with a ratiometric pair of calcium indicators, OGB-1-AM (2 μM, Invitrogen) and FR-AM (2.5 μM, Invitrogen), as described previously (Akiyama et al., 2009). Within each ROI on a growth cone, the emission ratio ($F_{OGB\text{-}1}/F_{FR}$, defined as R) was normalized to the baseline value (defined as R_{base}), and R/R_{base} (defined as R') was used a measure of cytosolic Ca^{2+} signals.

IP_3 imaging

Neurons were transfected with the IRIS-2.3 construct (Matsu-ura et al., 2019) using Nucleofector (Lonza) according to the manufacturer's protocols. The donor (EGFP) of IRIS-2.3 was excited with 488 nm light, and fluorescence images of EGFP and HaloTag®-TMR were acquired simultaneously with a CCD camera (ImagEM, Hamamatsu Photonics) after the dual-color image was split with an emission splitter. Because FRET efficiency from EGFP to HaloTag®-TMR decreases on IP_3 binding to IRIS-2.3, we calculated the inverse FRET ratio, i.e., the ratio of EGFP emission compared to TMR emission (F_{EGFP}/F_{TMR}, defined as R_{FRET}). Within each ROI, the averaged R_{FRET} was normalized to the baseline value (defined as $R_{FRET\text{-}base}$), and $R_{FRET}/R_{FRET\text{-}base}$ (defined as R') was used a measure of IP_3 levels.

Immunohistochemistry

The hindpaws of postnatal day 0 mice were collected in ice-cold PBS and fixed in 4% paraformaldehyde overnight. Tissue sections were made on a vibratome at 40 μm thickness and collected in regular PBS. From the blocking step onwards, high saline buffer (HSB: 500 mM

NaCl, 9.2 mM NaH_2PO_4, 12.5 mM Na_2HPO_4) was used to minimize background staining (Ramos-Vara, 2005). The sections were incubated overnight at 4ºC with primary antibodies against NGF (polyclonal rabbit, 1/500; EMD Millipore/Chemicon), TrkA (polyclonal goat, 1/100; R&D), GFP (monoclonal rat, 1/2000; Nacalai Tesque). On the next day, the sections were incubated in Alexa Fluor dye-conjugated secondary antibodies (1/500; Molecular Probes/ThermoFisher).

Whole-mount immunofluorescence and three-dimensional reconstruction

The hindpaw planta of postnatal day 0 mice were stained and tissue cleared according to the iDISCO method (Renier et al., 2014; Takahashi et al., 2019) with some modifications. In brief, the tissue was fixed in 4% paraformaldehyde overnight, treated with methanol, blocked with normal horse serum and incubated with anti-rat TrkA (polyclonal goat, 1/100; R&D) and a secondary antibody conjugated with Alexa Fluor 594 (1/1000; Molecular Probes/ThermoFisher). The specimen was imaged using a 63x HC PL APO CS2 oil immersion objective lens on a TCS SP8 confocal microscope (Leica Microsystems) controlled by LASX software. Three-dimensional animations were constructed from captured image stacks using LASX software.

NGF knockdown

We used RNA interference to knock down NGF expression in the skin. The 29-mer shRNA targeted against the ngf gene was purchased from Origene (catalog# TG510273). The 29-mer shRNA against turbo-red fluorescence protein (tRFP; catalog#TR30017) was used as a negative control. The NGF-targeting sequence was 5'-TGTGCTCAGCAGGAAGGCTACAAGAAGAG-3'. The negative control sequence was 5'-CTTCAAGACCACATACAGATCCAAGAAAC-3'. The shRNA cassette containing the U6 promoter, the shRNA hairpin and the termination sequence (TTTTTT) was sub-cloned into the tol2 plasmid (kind gift from Dr. Y. Takahashi, Kyoto University, Japan) (Sato et al., 2007). This is a transposon-donor plasmid harboring the Tol2 construct containing the CAG promoter and EGFP gene. Cotransfection with the transposase plasmid allowed long-term expression of NGF shRNA.

The effect of NGF knockdown was confirmed in primary cultures of skin keratinocytes transfected with the tol2 plasmid for NGF-EGFP expression. The plasmid encodes for a protein, in which NGF in its N-terminus is fused with EGFP via a linker sequence of ADPPVAT.

The shRNA plasmids were delivered into hindpaw skin epidermal cells via *in utero* electroporation, using previously established methods (Chan et al., 2019; Fukuchi-Shimogori and Grove, 2001; Matsui et al., 2011) with modifications for skin transfection. Briefly, a pregnant mouse was anesthetized with medetomidine, midazolam, and butorphanol. For each embryo (embryonic day 13 to 14), a mixture of 1 µl of 3 µg/µl shRNA plasmid and 1 µl of 1 µg/µl transposase plasmid was injected into the intra-amniotic space between the body and the right

hindpaw. Immediately, the embryo was electroporated using a protocol recommended by the manufacturer (Nepa Gene). The positive pole of pad platinum electrodes was placed on the dorsal surface of embryo's right hindpaw, and the negative pole on the left side of its body. Then, square pulses of 45-V amplitude and 50-ms pulse duration were administrated.

Quantification of axon morphology

To compare WT and R3KO TrkA axon morphologies, axons residing in the medial hind paw just caudal to the walking pad were included in the quantification. This is because axon morphologies in this region are the most consistent across animals. For quantification on a confocal microscopic image, we first defined the start and end points of each axon segment to be included in the analysis. The start was defined as the point where an axon crosses the boundary between the epidermal basal layer and the stratum spinosum that can be easily identified by NGF immunofluorescence. The end was defined as the distal tip of that axon. Then, we measured the length of each axon segment and the straight-line distance between the two ends of that segment, using the NeuronJ Plugin in ImageJ (Meijering et al., 2004). Axon morphologies were represented by the curviness index that was defined as the segment length divided by the linear distance between the two ends of that segment.

In experiments designed to examine the effect of NGF downregulation on the curviness index of TrkA axons, an epidermal area containing a cluster of more than three EGFP-positive cells was defined as an EGFP-positive area. Axons coursing within or in direct contact with this area were categorized as those 'within EGFP area'. For comparison, equal numbers of axons on each outside of the EGFP-positive area were categorized as those 'outside EGFP area'. For example, when three axons were found within EGFP area, three axons on the left and three axons on the right in the immediate neighborhood were included in the category of axons outside EGFP area, giving 3 test readings and 6 control readings of the curviness index.

Selection of axons and determination of the curviness index were performed by a researcher who was blind to mouse genotypes and treatment conditions.

Statistical analysis

All data are expressed as the mean ± SEM. Statistical analysis was performed using GraphPad Prism 7 (GraphPad Software). Each dataset was tested for normality by D'Agostino and Pearson omnibus or Shapiro-Wilk test. For analysis between two groups, normally distributed data were tested for equality of variances by F-test followed by paired *t* test or student's *t* test. Non-normally distributed data were analyzed by Wilcoxon matched pairs signed rank test. For analysis of three or more groups, normally distributed data were analyzed by Dunnett's multiple comparison test. All tests were two-tailed, and $P < 0.05$ was considered to be statistically significant.

Supplemental References

Barker, P.A., Lomen-Hoerth, C., Gensch, E.M., Meakin, S.O., Glass, D.J., Shooter, E.M. (1993). Tissue-specific alternative splicing generates two isoforms of the trkA receptor. J Biol Chem *268*,15150-15157.

Chan, C., Kamiguchi, H., and Shimogori, T. (2019). Spatially restricted long-term transgene expression in the developing skin used for studying the interaction of epidermal development and sensory innervation. Dev Growth Differ *61*, 276-282.

Fukuchi-Shimogori, T., and Grove, E.A. (2001). Neocortex patterning by the secreted signaling molecule FGF8. Science *294*, 1071-1074.

Futatsugi, A., Nakamura, T., Yamada, M.K., Ebisui, E., Nakamura, K., Uchida, K., Kitaguchi, T., Takahashi-Iwanaga, H., Noda, T., Aruga, J.*, et al.* (2005). IP_3 receptor types 2 and 3 mediate exocrine secretion underlying energy metabolism. Science *309*, 2232-2234.

Hong, K., Nishiyama, M., Henley, J., Tessier-Lavigne, M., and Poo, M. (2000). Calcium signalling in the guidance of nerve growth by netrin-1. Nature *403*, 93-98.

Matsui, A., Yoshida, A.C., Kubota, M., Ogawa, M., and Shimogori, T. (2011). Mouse in utero electroporation: controlled spatiotemporal gene transfection. J Vis Exp.

Matsumoto, M., Nakagawa, T., Inoue, T., Nagata, E., Tanaka, K., Takano, H., Minowa, O., Kuno, J., Sakakibara, S., Yamada, M.*, et al.* (1996). Ataxia and epileptic seizures in mice lacking type 1 inositol 1,4,5-trisphosphate receptor. Nature *379*, 168-171.

Meijering, E., Jacob, M., Sarria, J.C., Steiner, P., Hirling, H., and Unser, M. (2004). Design and validation of a tool for neurite tracing and analysis in fluorescence microscopy images. Cytometry A *58*, 167-176.

Otsu, H., Yamamoto, A., Maeda, N., Mikoshiba, K., and Tashiro, Y. (1990). Immunogold localization of inositol 1, 4, 5-trisphosphate ($InsP_3$) receptor in mouse cerebellar Purkinje cells using three monoclonal antibodies. Cell Struct Funct *15*, 163-173.

Ramos-Vara, J.A. (2005). Technical aspects of immunohistochemistry. Vet Pathol *42*, 405-426.

Renier, N., Wu, Z., Simon, D.J., Yang, J., Ariel, P., and Tessier-Lavigne, M. (2014). iDISCO: a simple, rapid method to immunolabel large tissue samples for volume imaging. Cell *159*, 896-910.

Sato, Y., Kasai, T., Nakagawa, S., Tanabe, K., Watanabe, T., Kawakami, K., and Takahashi, Y. (2007). Stable integration and conditional expression of electroporated transgenes in chicken embryos. Dev Biol *305*, 616-624.

Takahashi, S., Ishida, A., Kubo, A., Kawasaki, H., Ochiai, S., Nakayama, M., Koseki, H., Amagai, M., and Okada, T. (2019). Homeostatic pruning and activity of epidermal nerves are dysregulated in barrier-impaired skin during chronic itch development. Sci Rep *9*, 8625.

Wada, F., Nakata, A., Tatsu, Y., Ooashi, N., Fukuda, T., Nabetani, T., and Kamiguchi, H. (2016). Myosin Va and Endoplasmic Reticulum Calcium Channel Complex Regulates Membrane Export during Axon Guidance. Cell Rep *15*, 1329-1344.